Electronic Supplementary Material (ESI) for CrystEngComm.

Supplementary Msterials

Cd(II) Coordination Polymers Constructed from Tris-pyridyl-tris-amide and Polycarboxylic acid: Synthesis, Structures and Sensing Properties

Chia-Ling Chen, Song-Wei Wang, Shih-Ying Zhong and Jhy-Der Chen*

Fig. S1. IR spectrum of complex **1**.

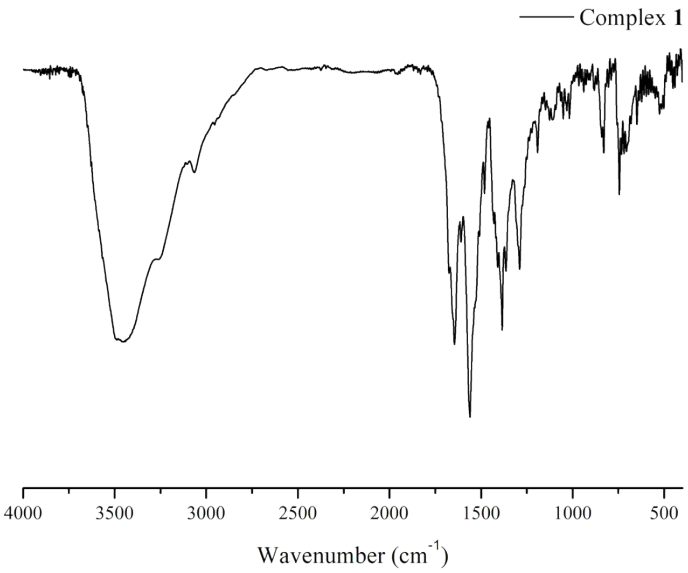

Fig. S2. IR spectrum of complex **2**.

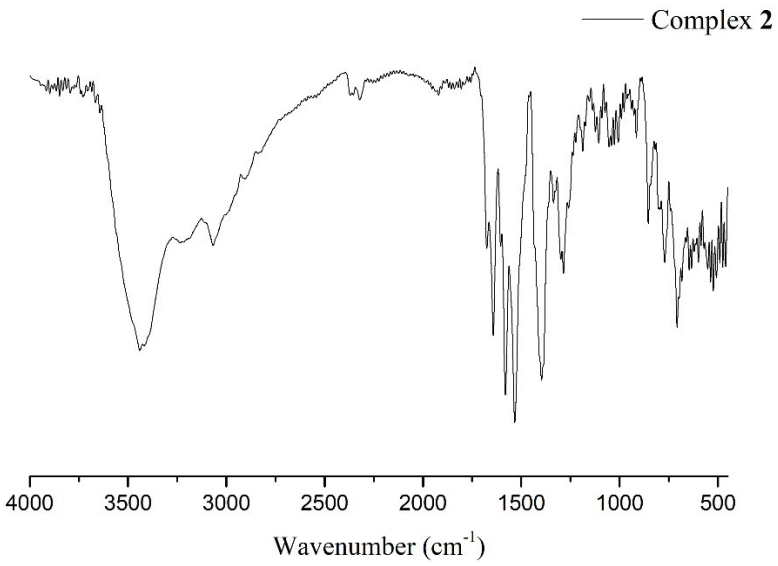

Fig. S3. IR spectrum of complex **3**.

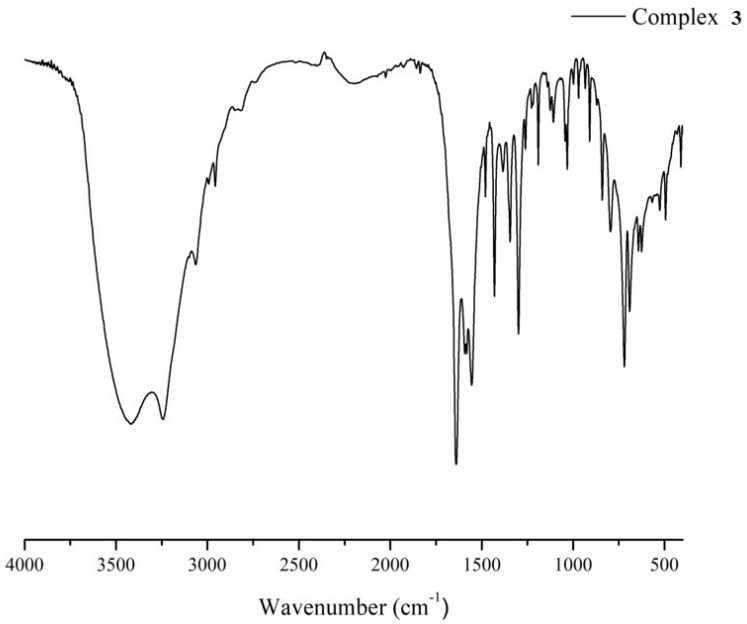

Fig. S4. The PXRD patterns of complex **1**.

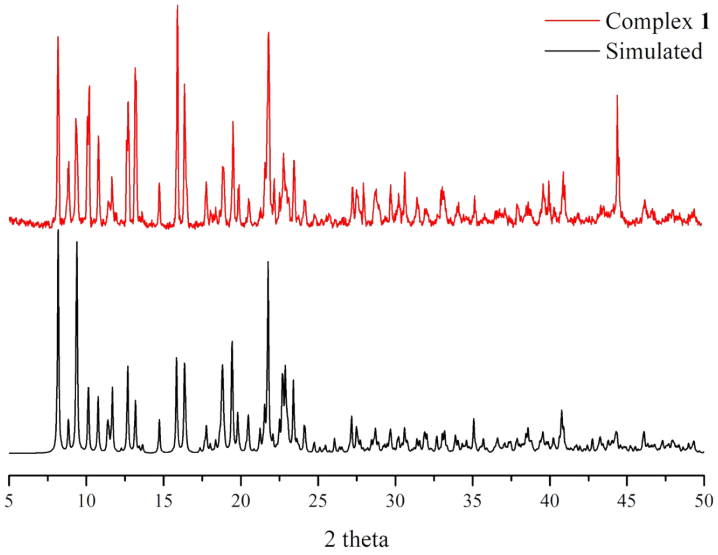

Fig. S5. The PXRD patterns of complex **2**.

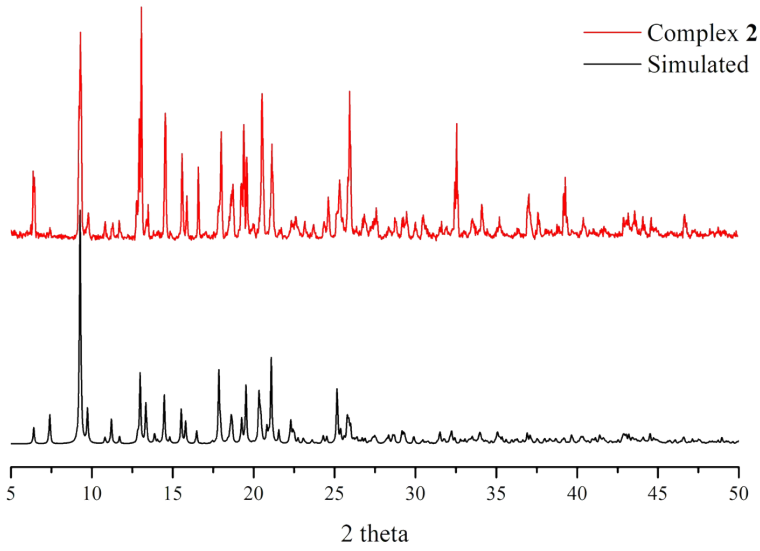

Fig. S6. The PXRD patterns of complex **3**.

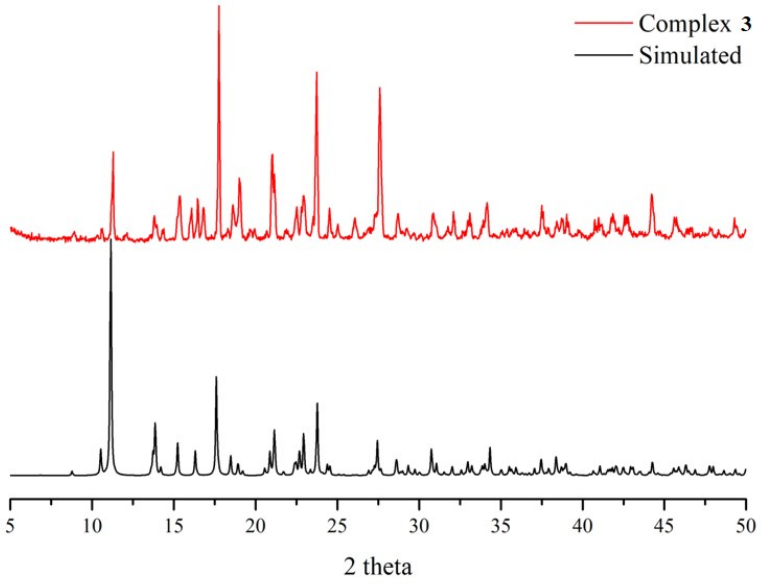

Fig. S7. TGA curve of complex **1**.

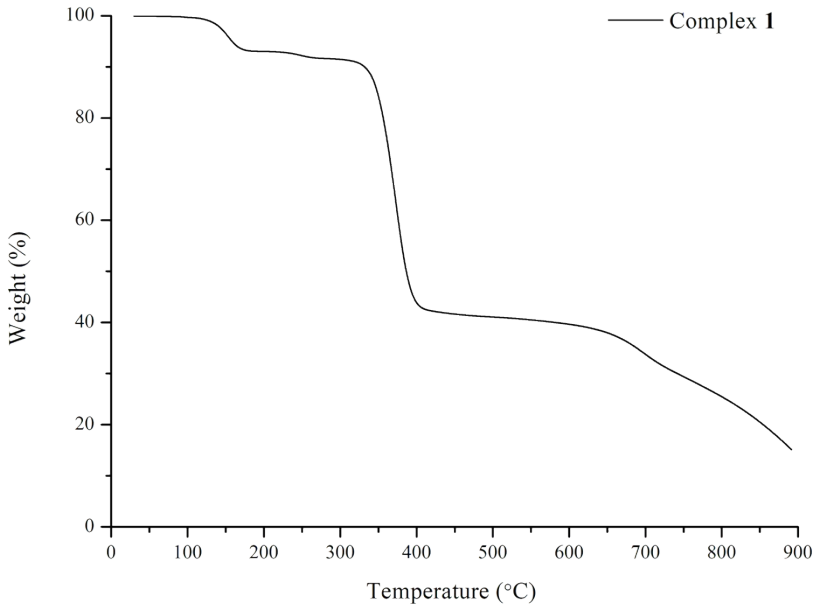

Fig. S8. TGA curve of complex **2**.

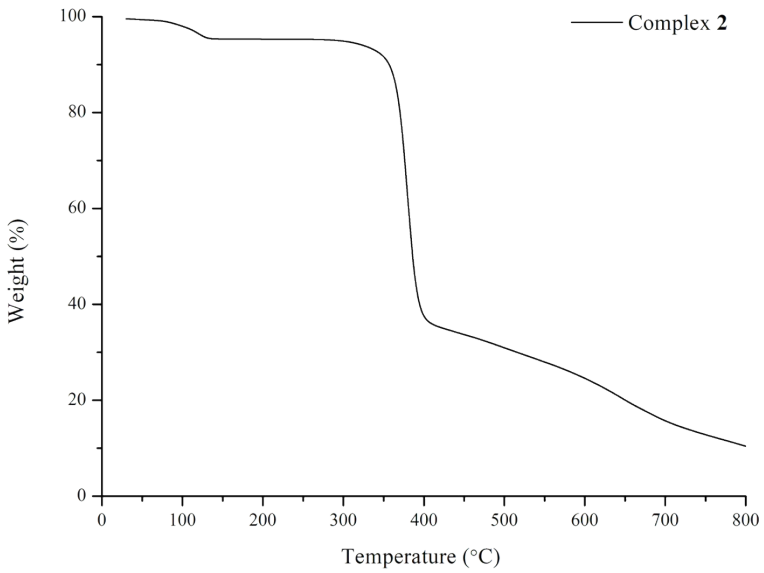

Fig. S9. TGA curve of complex **3**.

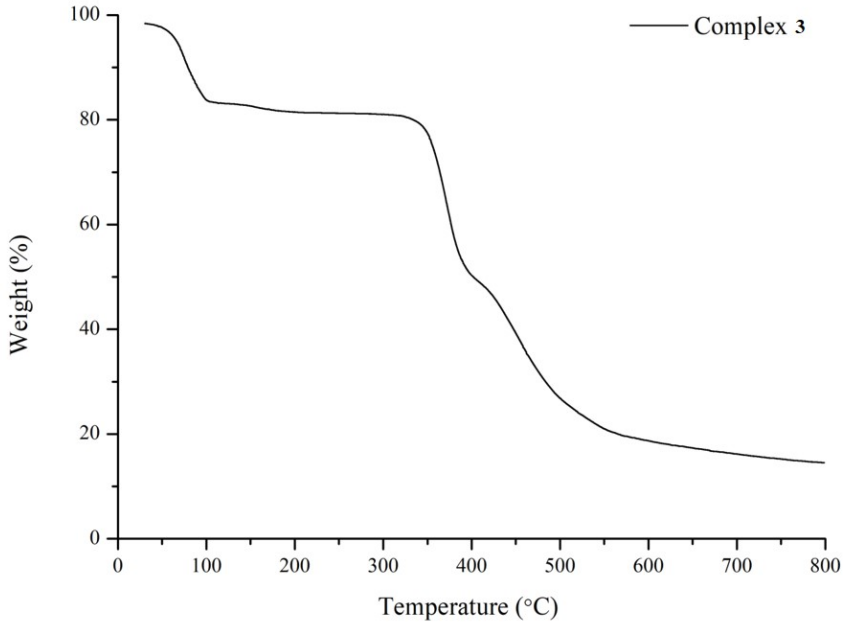

Fig. S10. The PXRD patterns of complex **1** before and after immersion in different solvents.

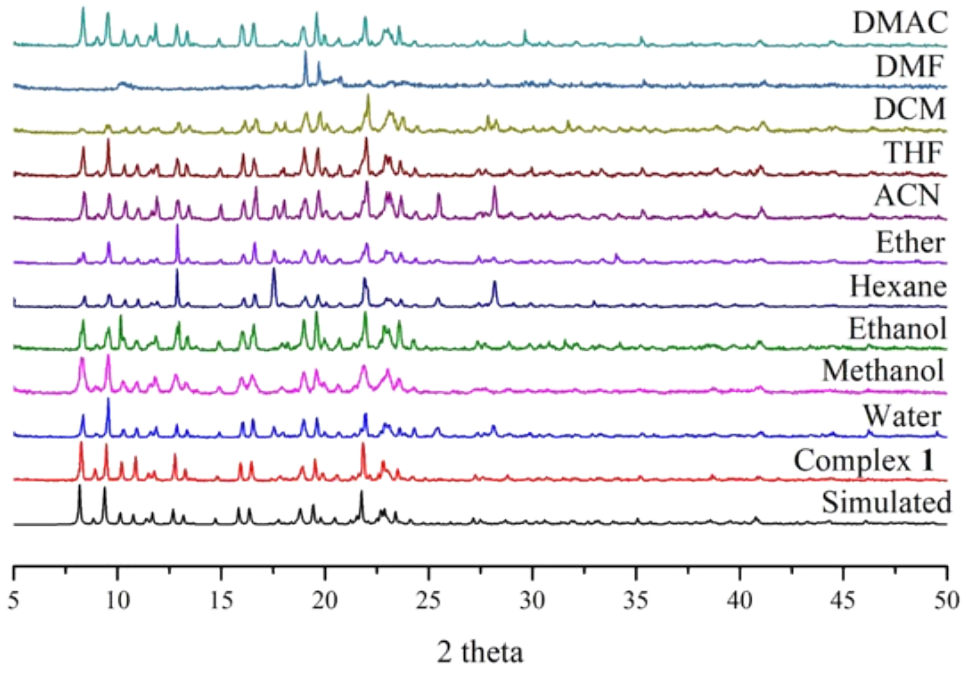

Fig. S11. The PXRD patterns of complex **2** before and after immersion in different solvents.

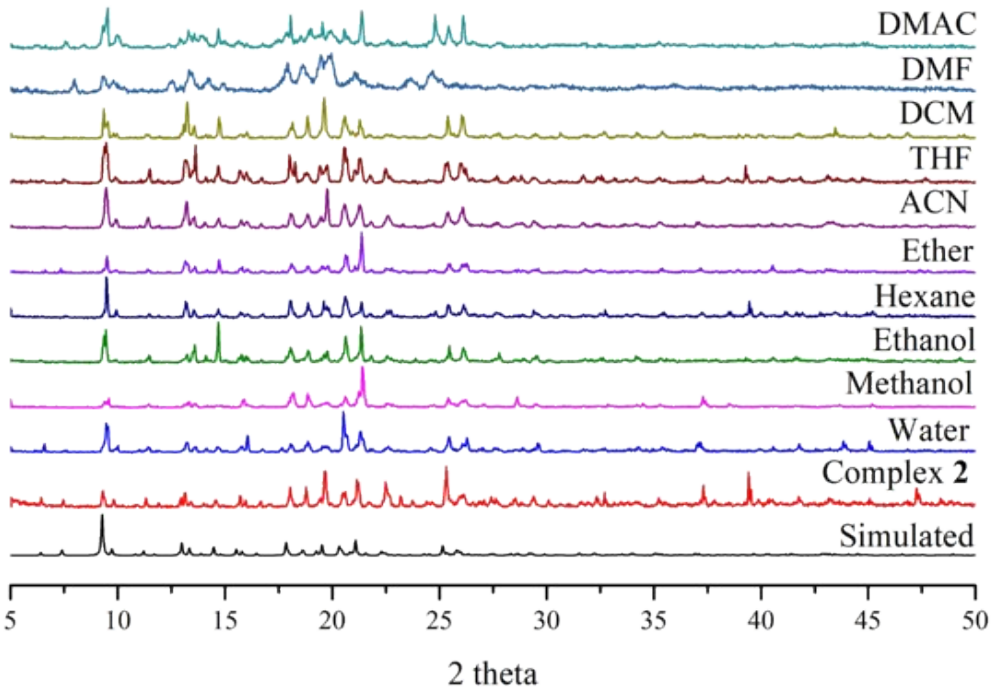

Fig. S12. The photoluminescence spectra of **L**.

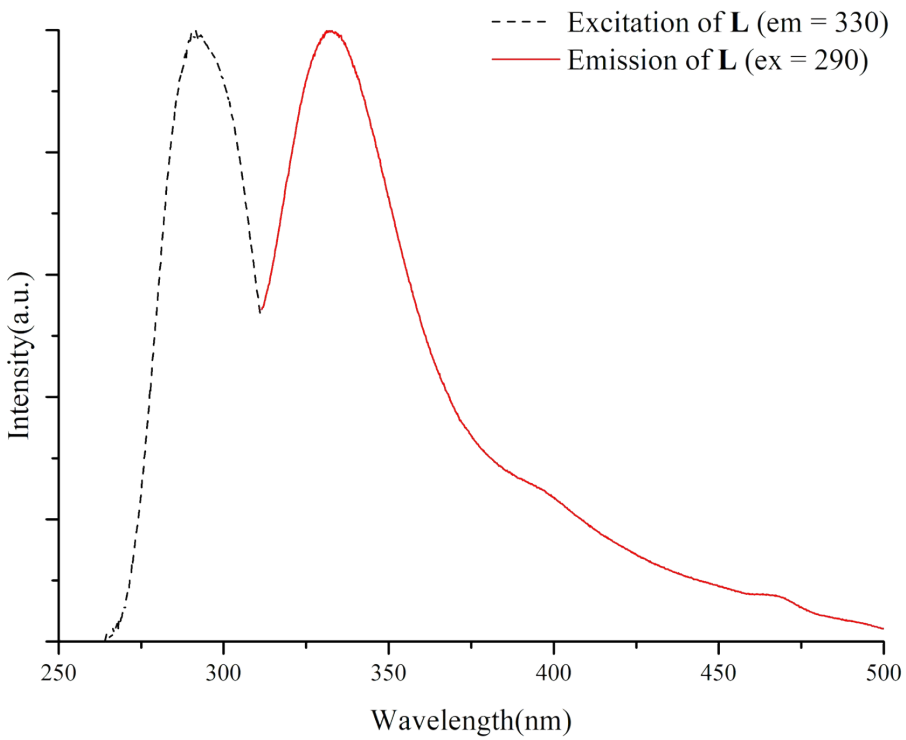

Fig. S13. The photoluminescence spectra of 1,4-H_2BDC.

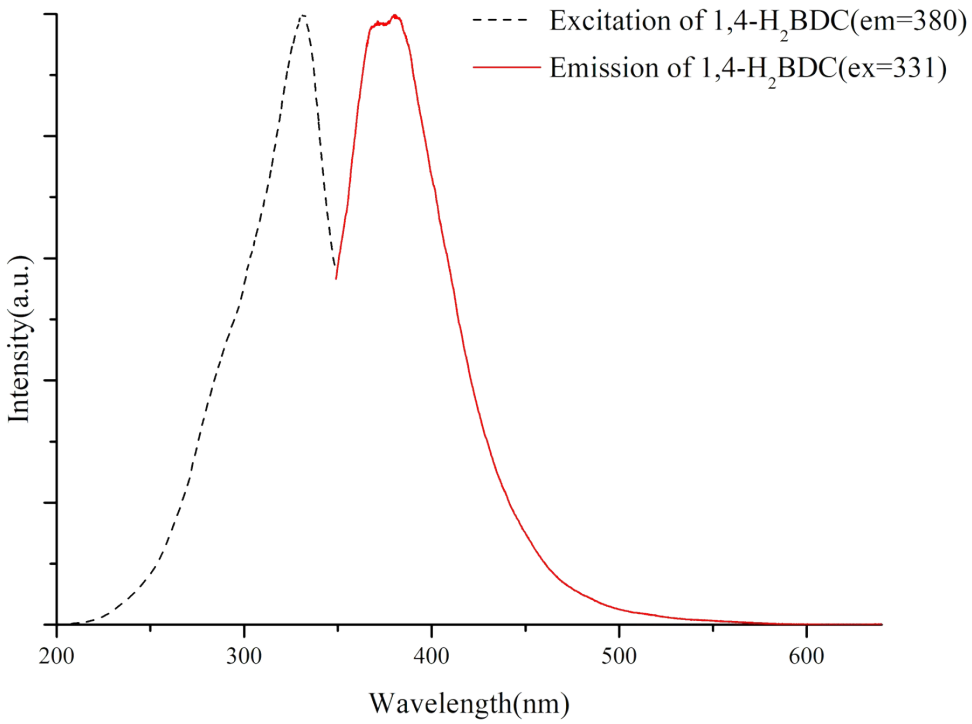

Fig. S14. The photoluminescence spectra of 4,4'-H_2BDC.

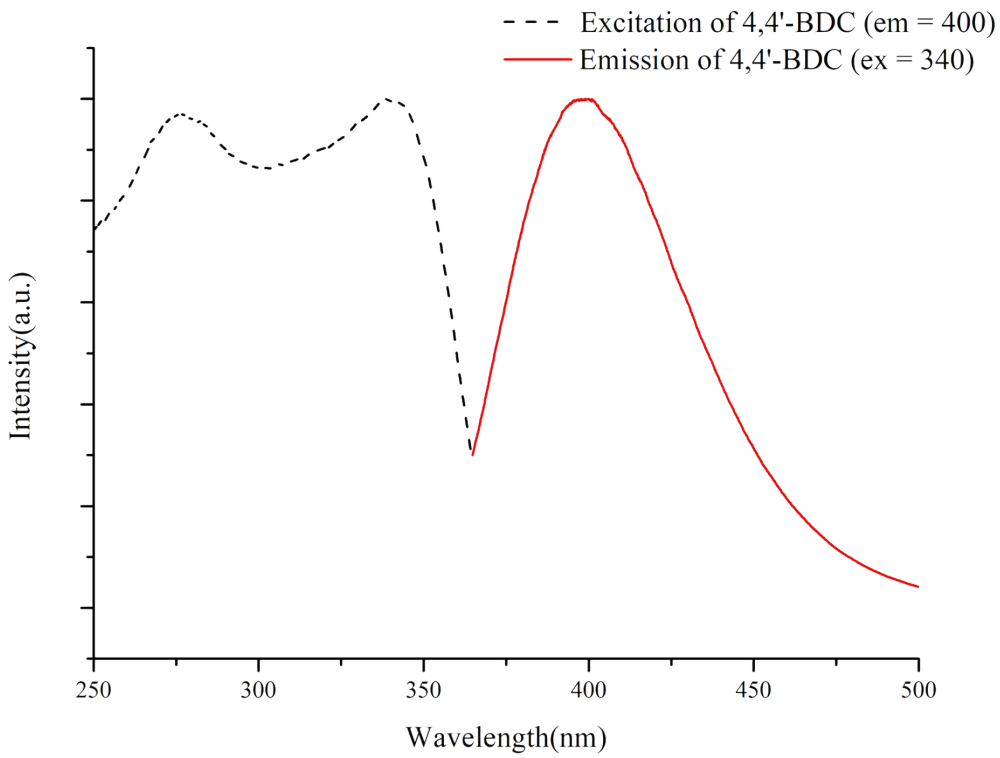

Fig. S15. The photoluminescence spectra of complex **1**.

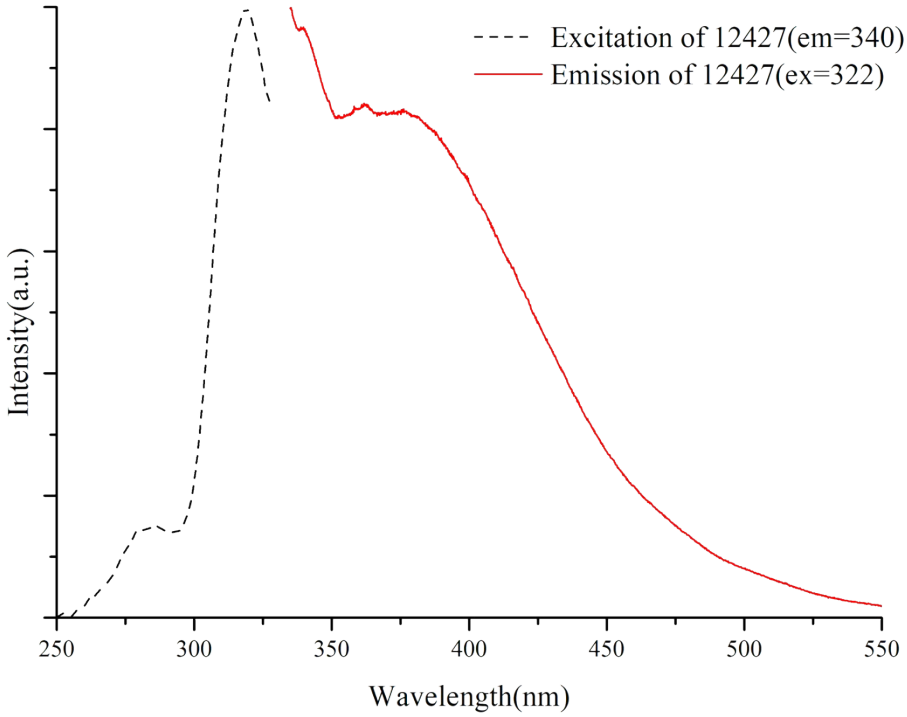

Fig. S16. The photoluminescence spectra of complex **2**.

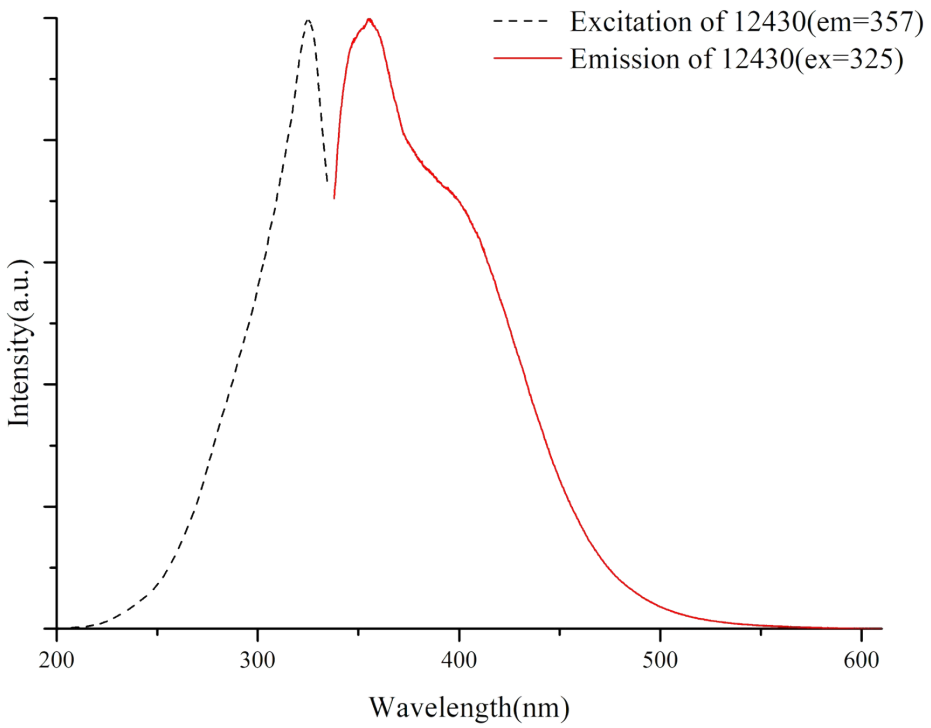

Fig. S17. The solid-state luminescence spectra of complex **1** before and after immersion into different metal cations.

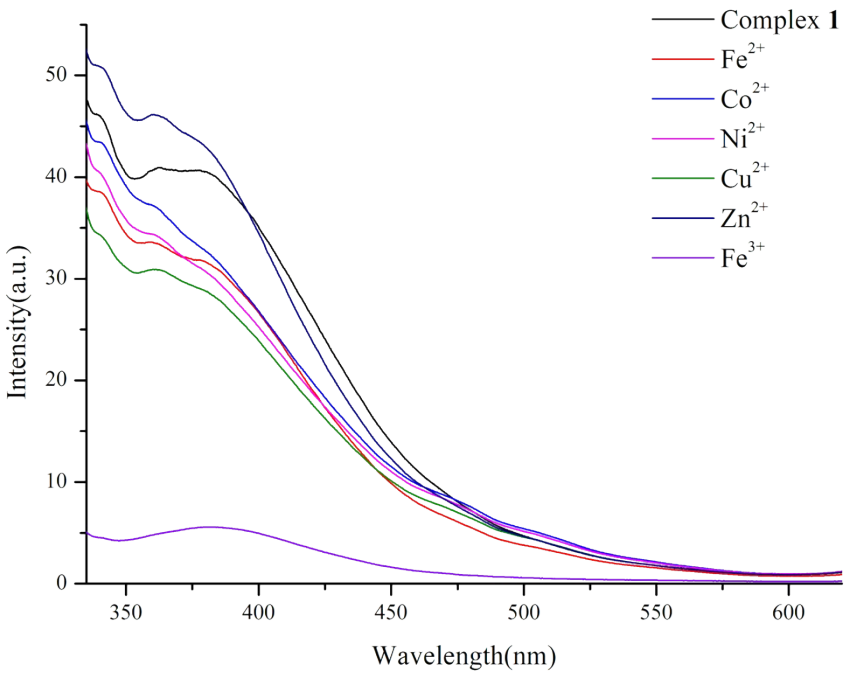

Fig. S18. The solid-state luminescence spectra of complex **2** before and after immersion into different metal cations.

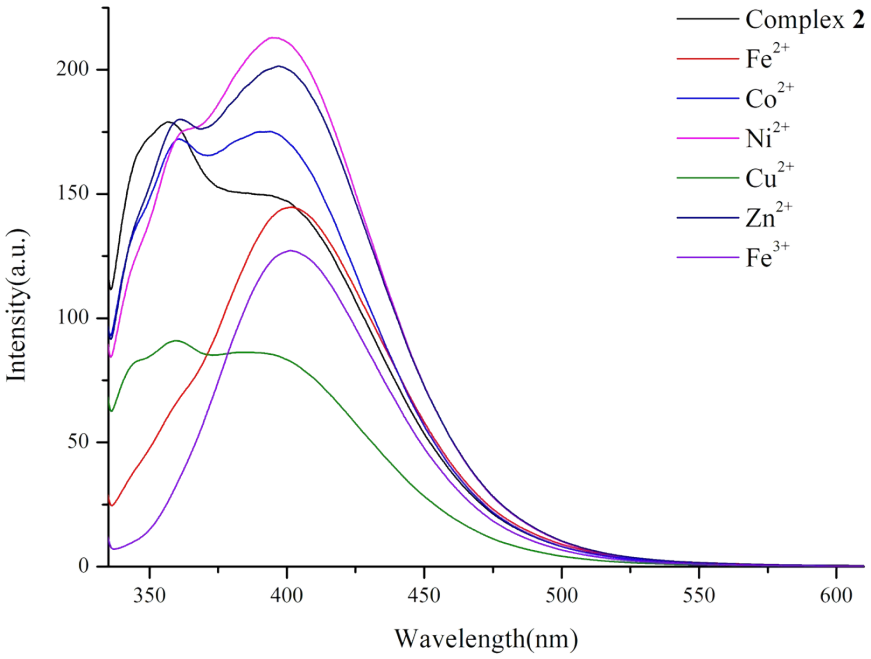

Fig. S19. The emission spectra of complex **1** in different concentrations of Fe^{3+} ion.

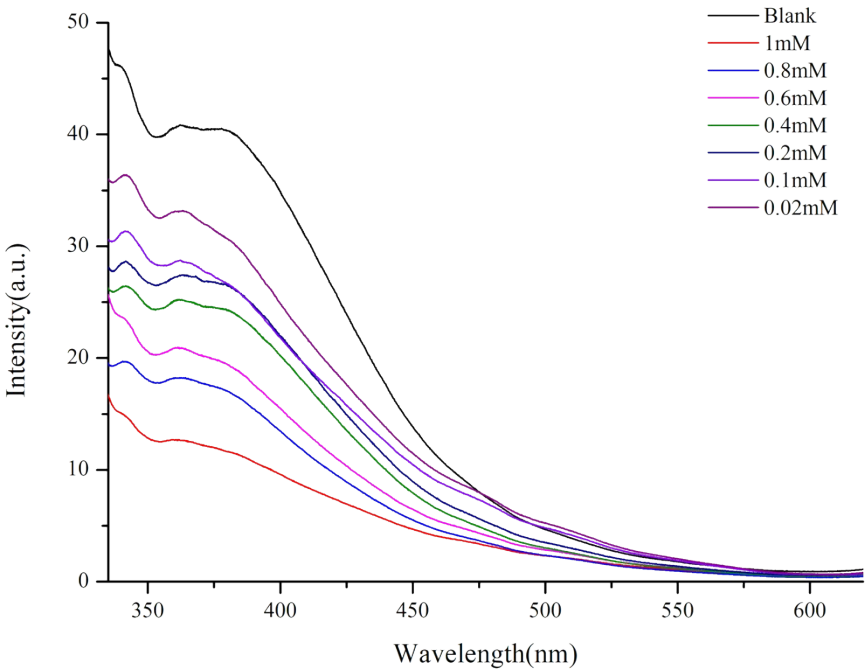

Fig. S20. The emission spectra of complex **2** in different concentrations of Fe^{3+} ion.

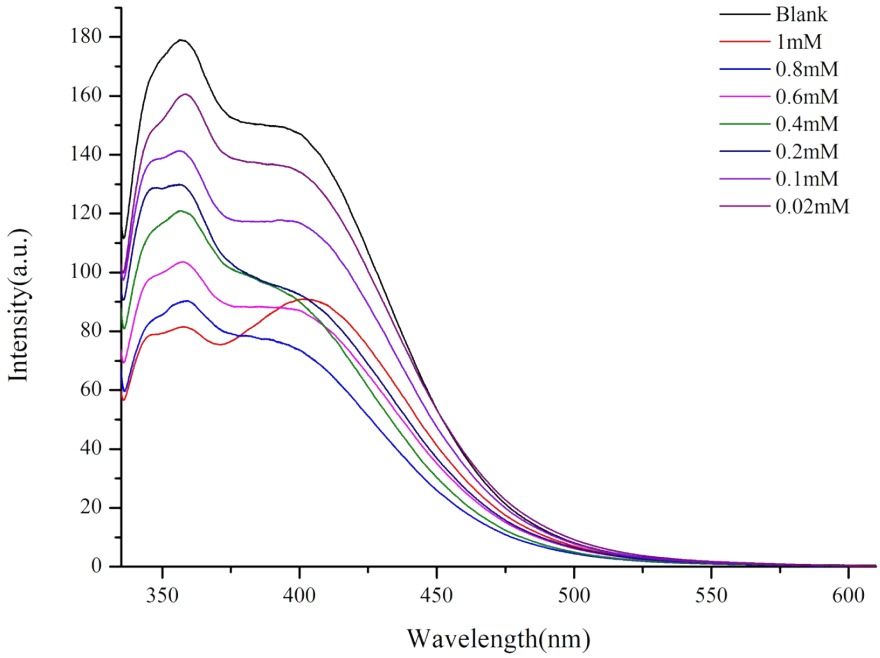

Fig. S21. PXRD patterns for complex **1** after Fe^{3+} sensing for five cycles.

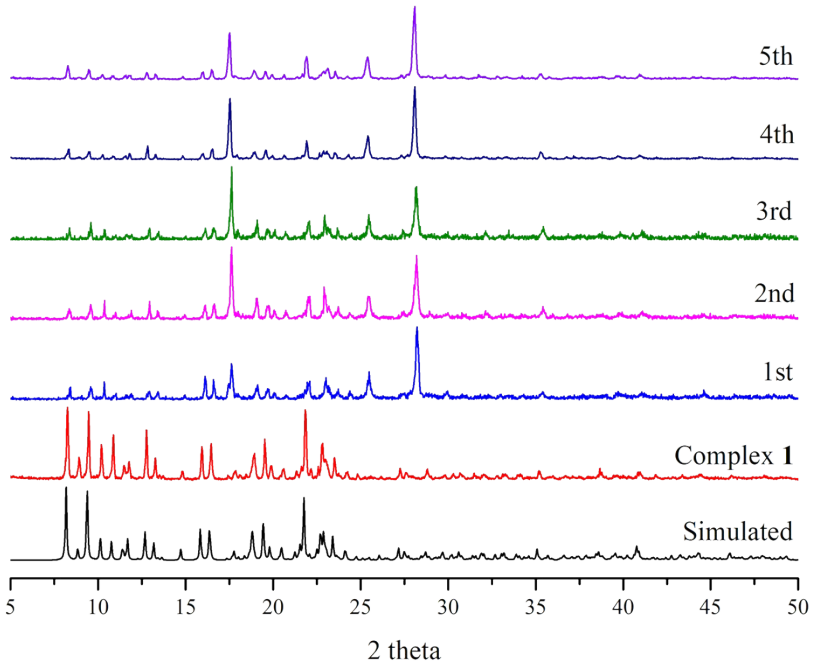

Fig. S22. PXRD patterns for complex **2** after Fe^{3+} sensing for five cycles.

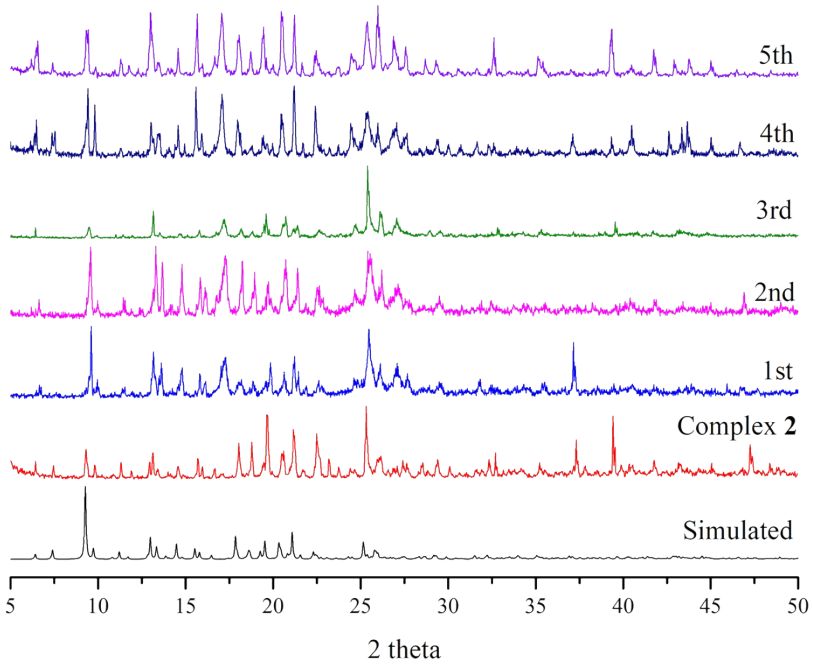

Fig. S23. The PXRD patterns of complex **1** before and after immersion in different metal cations.

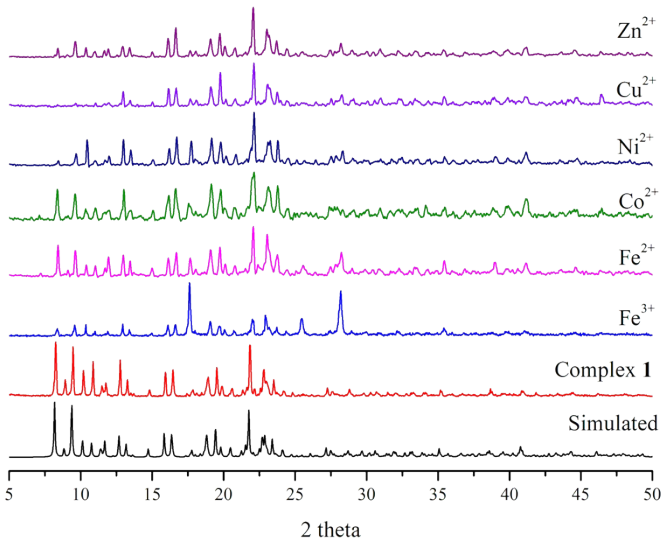

Fig. S24. The PXRD patterns of complex **2** before and after immersion in different metal cations.

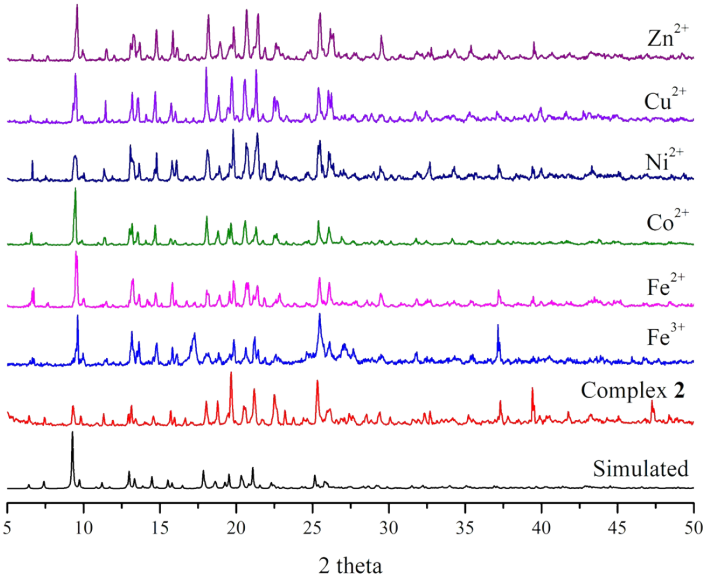

Fig. S25. UV-vis absorption spectra of Fe^{3+} and the excitation and emission spectra of (a) **1** and (b) **2**.

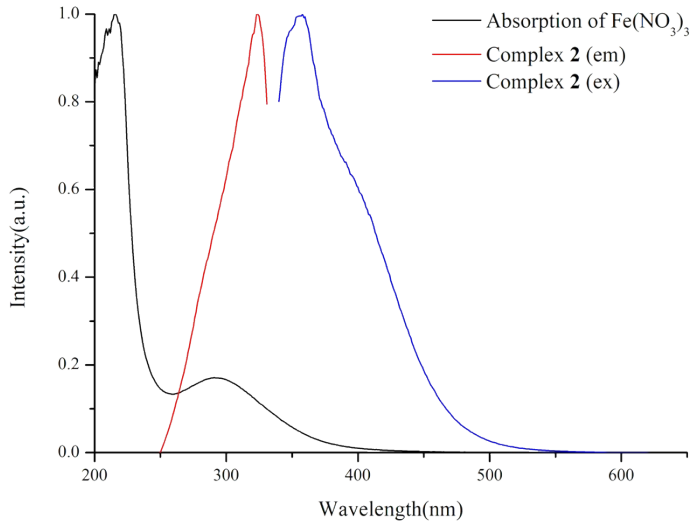

(b)

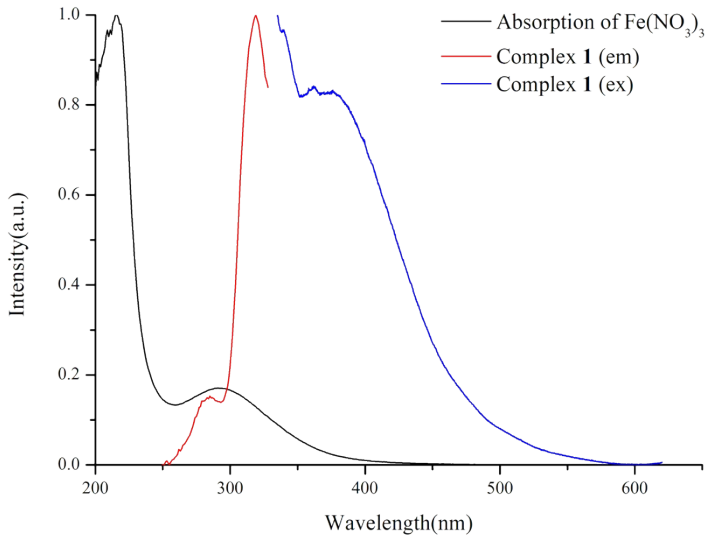

(a)

Fig. S26. The EDX data of complex **1**. (a) The selected part for point scan. (b) The result of point scan. (c) The element mapping scan of Fe^{3+}. (d) The element percentage analysis of point scan.

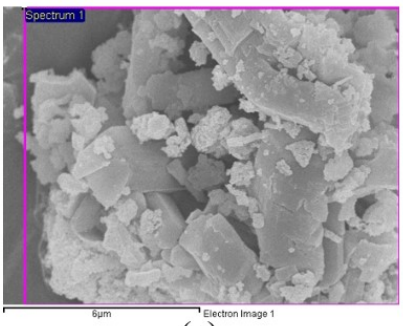

(a)

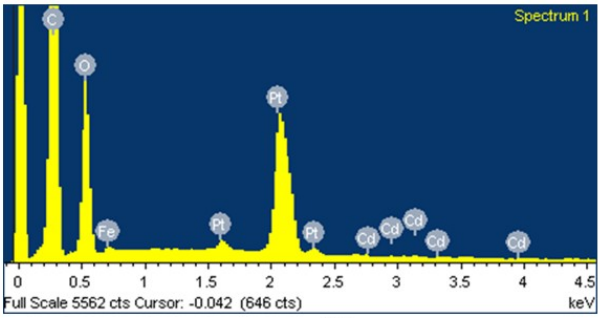

(b)

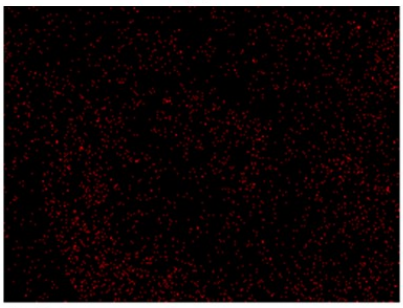

(c)

Element	Weight (%)	Percentage (%)
C K	49.47	75.97
O K	19.99	23.05
Fe L	2.67	0.88
Cd L	0.62	0.10

(d)

Fig. S27. The EDX data of complex **2**. (a) The selected part for point scan. (b) The result of point scan. (c) The element mapping scan of Fe^{3+}. (d) The element percentage analysis of point scan.

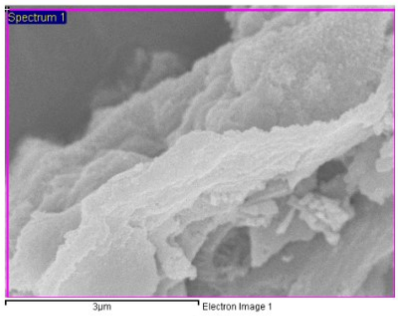

(a)

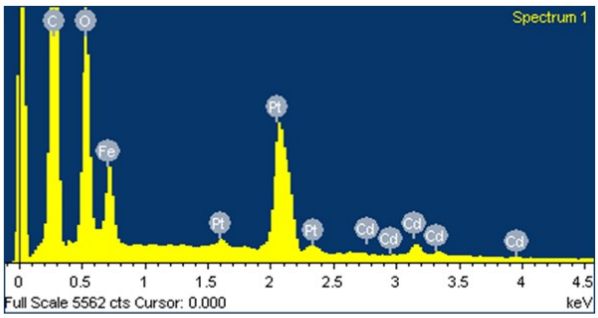

(b)

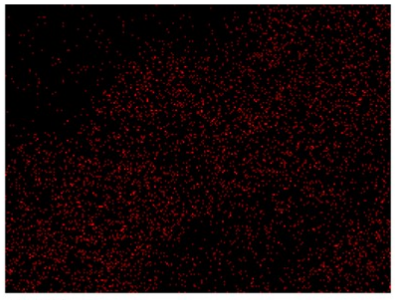

(c)

Element	Weight (%)	Percentage (%)
C K	38.66	67.49
O K	18.02	23.63
Fe L	22.40	8.41
Cd L	2.60	0.49

(d)

Fig. S28. IR spectra of **L**, 1,4-H_2BDC and complex **1** before and after immersion in Fe^{3+}.

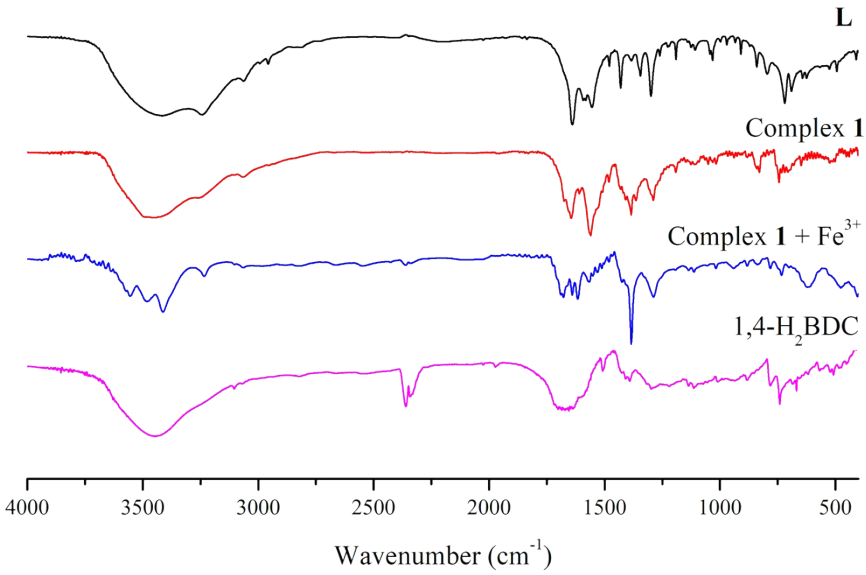

Fig. S29. IR spectra of **L**, 4,4'-H_2BDC and complex **2** before and after immersion in Fe^{3+}.

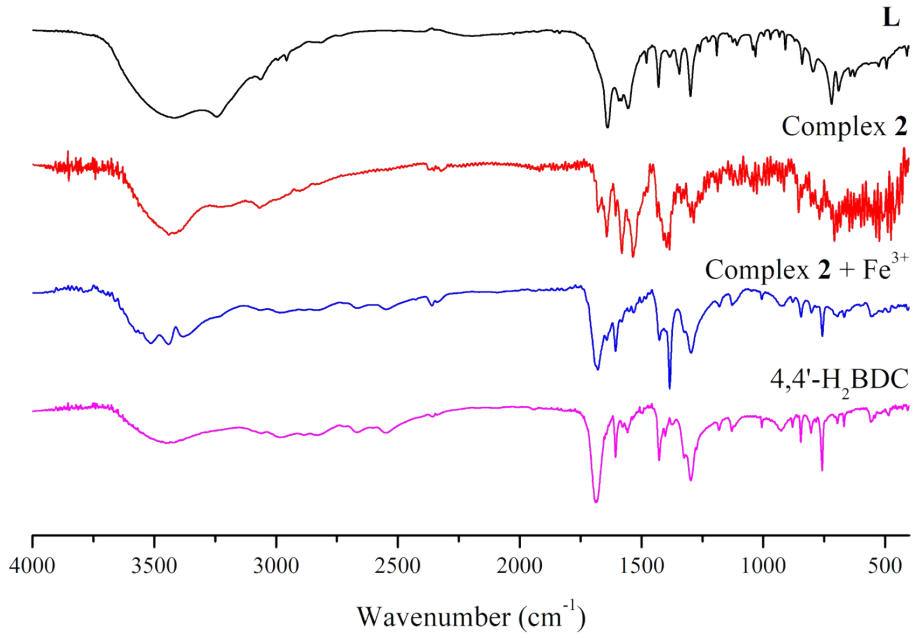

Fig. S30. Selected XPS patterns before and after addition of Fe^{3+} ion to complex **2**.

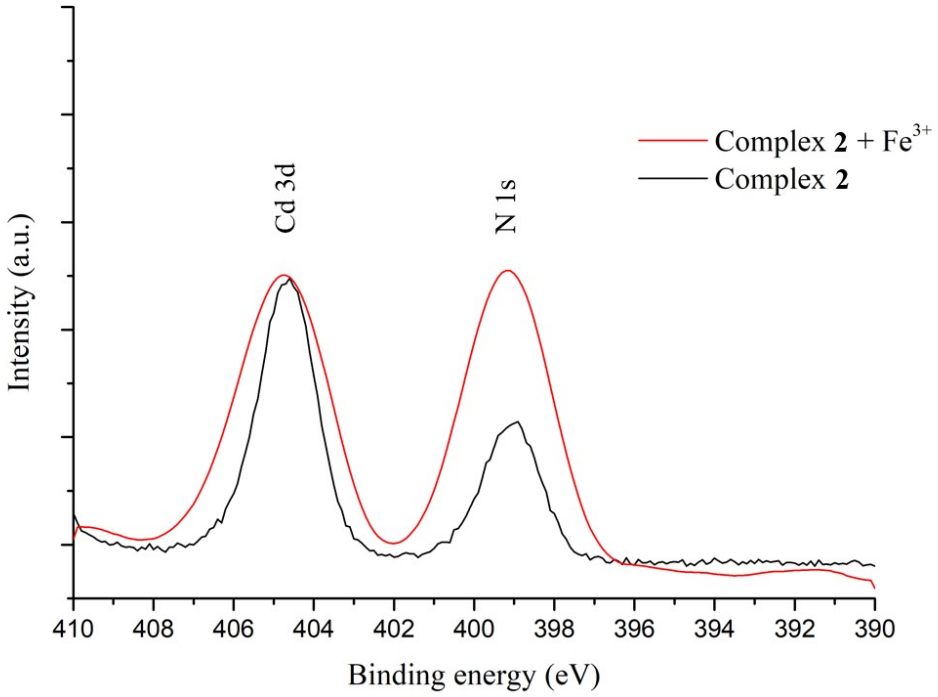

Fig. S31. Competitive sensing experiments in the presence of the other cations for complexes (a) **1** and (b) **2**.

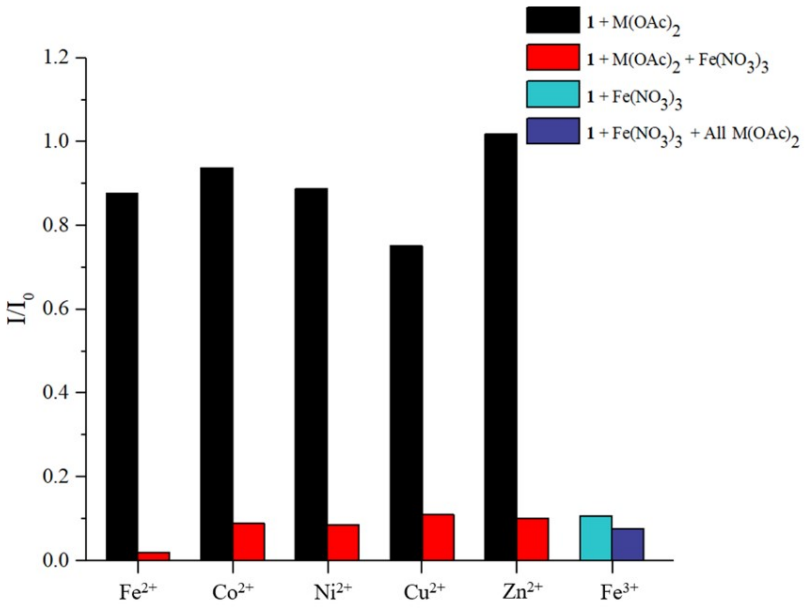
1 + M(OAc)2
1 + M(OAc)2 + Fe(NO3)3
1 + Fe(NO3)3
1 + Fe(NO3)3 + All M(OAc)2
I/I0
1.2
1.0
0.8
0.6
0.4
0.2
0.0
Fe2+
Co2+
Ni2+
Cu2+
Zn2+
Fe3+

(a)

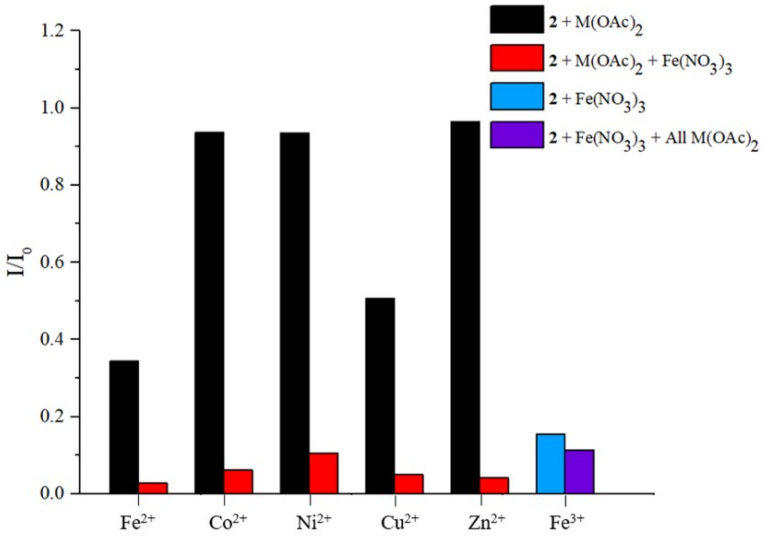
2 + M(OAc)2
2 + M(OAc)2 + Fe(NO3)3
2 + Fe(NO3)3
2 + Fe(NO3)3 + All M(OAc)2
I/I0
1.2
1.0
0.8
0.6
0.4
0.2
0.0
Fe2+
Co2+
Ni2+
Cu2+
Zn2+
Fe3+

(b)

Fig. S32. (a) N_2 adsorption−desorption isotherms for complex **1**. (b) Pore-size distribution curve for complex **1**.

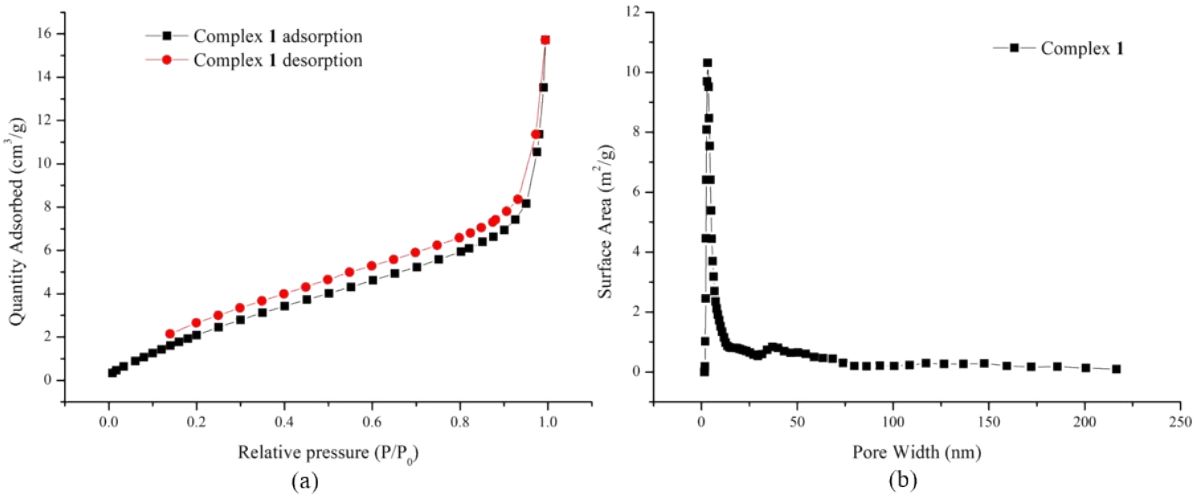

Fig. S33. (a) N_2 adsorption−desorption isotherms for complex **2**. (b) Pore-size distribution curve for complex **2**.

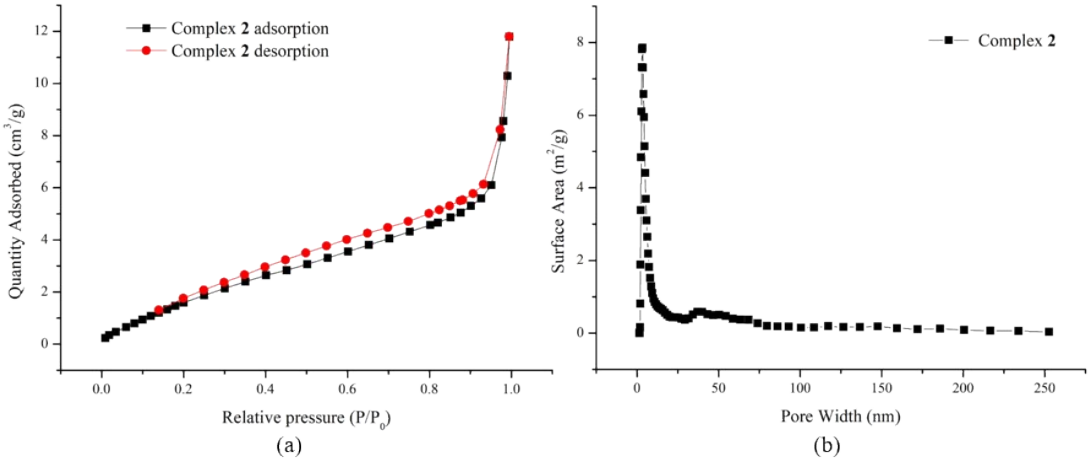

Fig. S34. PXRD patterns for complex **1** before and after N_2 adsorption and desorption.

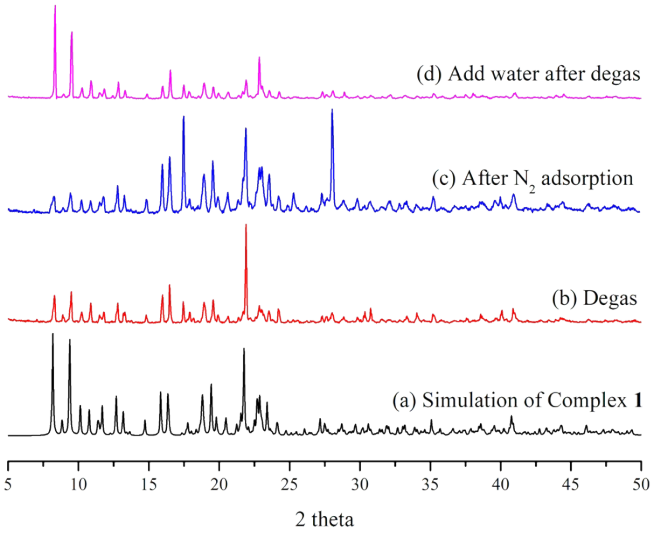

Fig. S35. PXRD patterns for complex **2** before and after N_2 adsorption and desorption.